High-Performance Solution-Processable Poly(p-phenylene vinylene)s for Air-Stable Organic Field-Effect Transistors

Breemen, Albert J.J.M. van; Herwig, Peter T.; Chlon, Ceciel H.T.; Sweelssen, Jörgen; Schoo, Herman F.M.; Benito, Estrella Mena; Leeuw, Dago M. de; Tanase, Christina; Wildeman, Jurjen; Blom, Paul W.M.

Published in:
Advanced Functional Materials

DOI:
10.1002/adfm.200400445

Publication date:
2005

FULL PAPER

ADVANCED FUNCTIONAL MATERIALS

High-Performance Solution-Processable Poly(*p*-phenylene vinylene)s for Air-Stable Organic Field-Effect Transistors

By *Albert J. J. M. van Breemen*,* *Peter T. Herwig*, *Ceciel H. T. Chlon*, *Jörgen Sweelssen*, *Herman F. M. Schoo*, *Estrella Mena Benito*, *Dago M. de Leeuw*, *Christina Tanase*, *Jurjen Wildeman*, and *Paul W. M. Blom*

The influence of the substitution pattern (unsymmetrical or symmetrical), the nature of the side chain (linear or branched), and the processing of several solution processable alkoxy-substituted poly(*p*-phenylene vinylene)s (PPVs) on the charge-carrier mobility in organic field-effect transistors (OFETs) is investigated. We have found the highest mobilities in a class of symmetrically substituted PPVs with linear alkyl chains (e.g., R^1, $R^2 = n\text{-}C_{11}H_{23}$, $R^3 = n\text{-}C_{18}H_{37}$). We have shown that the mobility of these PPVs can be improved significantly up to values of 10^{-2} $cm^2 V^{-1} s^{-1}$ by annealing at 110 °C. In addition, these devices display an excellent stability in air and dark conditions. No change in the electrical performance is observed, even after storage for thirty days in humid air.

1. Introduction

The use of solution-processable semiconductors in organic field-effect transistors (OFETs) and integrated circuits is of major importance for the commercialization of low-end, high-volume microelectronics. The main advantage of the use of solution-processable semiconducting polymers is their mechanical flexibility and ease of processing. Applications are foreseen in integrated circuits for disposable smart labels and transponders, field-effect transistors in pixel engines and integrated drivers of flexible displays, electronic paper, and as an active component in sensors or in polymeric solar cells.[1–3]

The benchmark of solution-processable polymeric semiconductors for OFETs are thiophene-containing polymers such as poly(3-hexyl thiophene)s, (P3HTs), poly(3″,4″-didecyl-2,2′;5′,2″-terthiophene) (PTT-10), and poly(3,3‴-didodecyl quaterthiophene)s (PQT-12s).

Typical field-effect mobilities for spin-coated films of amorphous, regiorandom P3HT are in the range of 10^{-5}–10^{-4} $cm^2 V^{-1} s^{-1}$.[4] A dramatic increase in mobility was observed by making use of supramolecular self-organization of highly regioregular head-to-tail P3HT. Typical values of 10^{-2} $cm^2 V^{-1} s^{-1}$ were achieved in these highly ordered films.[5,6] Despite these high mobilities, the use of P3HT in practical applications is hampered because of its limited stability in air.[7] Poly(thiophenes) with a better stability against oxidative doping were recently described by Ong et al.[8,9] These materials show mobilities of up to 10^{-1} $cm^2 V^{-1} s^{-1}$ after annealing and an enhanced stability in dry air.[10]

Poly(*p*-phenylene vinylene)s (PPVs) have found widespread use as electroluminescent materials in polymer light-emitting diodes (PLEDs). The first commercial application in which a PPV was used as the active material was launched in 2002.[11] For application in PLEDs, materials are optimized in order to obtain high electroluminescence efficiencies. It is well known that aggregate formation and excimer interactions lower the luminescence efficiency, and hence should be avoided, because of undesirable red-shifted emission bands and nonradiative relaxation pathways. Therefore, side chains are chosen in such a way (e.g., R^1–R^4 in NRS-PPV, Scheme 1) that aggregation is suppressed, resulting in completely amorphous materials. Charge-carrier mobilities of these PPVs in LEDs are low, typically about 10^{-7} $cm^2 V^{-1} s^{-1}$. However, recently,[12] it was shown that the mobility in a field-effect transistor (5×10^{-4} $cm^2 V^{-1} s^{-1}$) of such an amorphous PPV, viz. OC_1C_{10}–PPV (**4a**) is approximately three orders of magnitude larger than the mobility value obtained from hole-only diodes. Considering the fact that these PPVs were not optimized for charge transport, the mobility values are reasonable. This prompted us to evaluate new PPVs which are especially designed for use as charge-transport material in field-effect transistors.

For this work, different classes of easily accessible alkoxy-substituted PPVs were examined (see Table 1). The influence of the substitution pattern of the phenyl ring (unsymmetrical or symmetrical), the nature of the side chain (linear or branched), and the processing of the semiconductor on the field-effect mobility in OFETs was investigated.

[*] Dr. A. J. J. M. van Breemen, P. T. Herwig, C. H. T. Chlon, J. Sweelssen, Dr. H. F. M. Schoo
TNO Science and Industry
De Rondom 1
P.O. Box 6235, NL-5600 HE Eindhoven (The Netherlands)
E-mail: albert.vanbreemen@tno.nl
E. M. Benito, Dr. D. M. de Leeuw
Philips Research Laboratories
Professor Holstlaan 4, NL-5656 AA Eindhoven (The Netherlands)
C. Tanase, J. Wildeman, Prof. P. W. M. Blom
University of Groningen
Nijenborgh 4, NL-9747 AG Groningen (The Netherlands)

  DOI: 10.1002/adfm.200400445

ADVANCED FUNCTIONAL MATERIALS

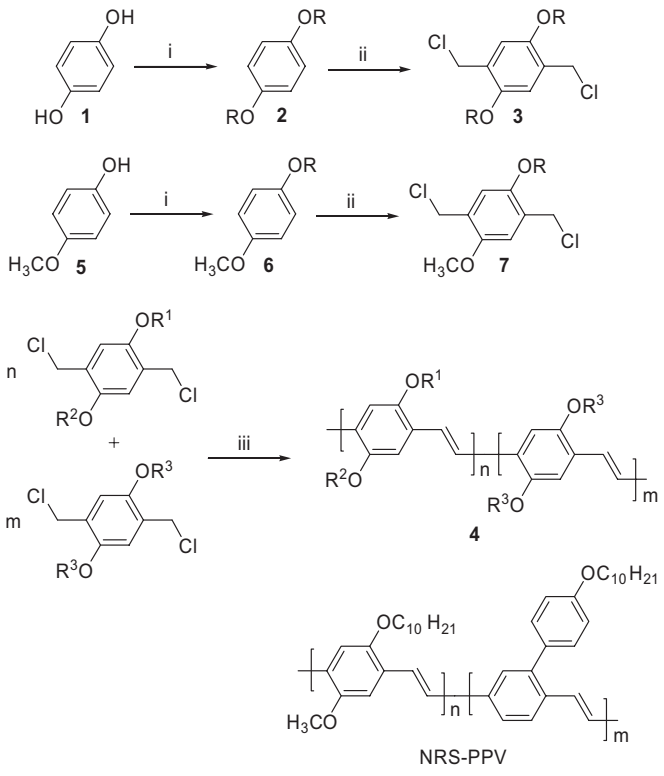

Scheme 1. Synthesis of alkoxy PPVs. i: RBr, KOH, DMSO, room temperature (rt); ii: $(CH_2O)_n$, HCl, Ac_2O, 1,4-dioxane, 70 °C; iii: KOtBu, 1,4-dioxane, 98 °C.

2. Results and Discussion

The two-step synthesis of monomers **3** and **7** is outlined in Scheme 1. Thus, alkylation of hydroquinone or *p*-methoxyphenol, respectively, yielded the bis(alkoxy)benzenes **2** and **6** in almost quantitative yield. These were subsequently treated with paraformaldehyde and hydrochloric acid, yielding the bis(chloromethyl) monomers **3** and **7**. Overall yield of this monomer synthesis was typically 60–65 %. Polymerization of the respective monomers was done following a modified Gilch[13] dehydrohalogenation procedure and in-situ elimination using an excess base in refluxing 1,4-dioxane.[14] The crude polymers were carefully purified by means of repetitive precipitation to afford PPVs **4** in 55–70 % yield. Despite the high molecular weights of these polymers (weight-average molecular weight, $M_w = 1.3 \times 10^5$–1.4×10^6 g mol^{-1}), all (co)polymers are nicely soluble in common organic solvents (e.g., ≥5 mg mL^{-1} in toluene, xylene, and chlorobenzene) and can therefore be processed into homogeneous thin films by standard solution-based coating processes like spin-coating or knife-casting. Analytical data are in agreement with the proposed structure and composition. The amount of tolane-bis-benzyl (TBB)[15] moieties, the major polymerization defect in the Gilch procedure, was determined using ^{1}H NMR spectroscopy. Except for NRS-PPV (3–4 %), all other derivatives have a TBB content of 1.5–2.5 %.

In order to study the electrical transport in field-effect transistors, the respective PPVs were spin-coated from chloroben-

Table 1. Composition and field-effect mobility of PPVs under investigation.

							Molecular weight [a] [g mol^{-1}]		μ [b] [cm^2 V^{-1} s^{-1}]	
	Polymer	R^1	R^2	R^3	*n*	*m*	M_w	M_n	Pristine	After annealing [c]
Class 1	NRS						7.5×10^5	2.6×10^5	1×10^{-4}	no improvement
unsymmetrically substituted PPVs	**4a**	CH_3	$C_{10}H_{21}$ [d]		1		8.2×10^5	2.3×10^5	4×10^{-4}	no improvement
	4b	CH_3	C_8H_{17} [e]		1		2.1×10^5	6.3×10^4	5×10^{-4}	no improvement
	4c	CH_3	*n*-$C_{18}H_{37}$		1		1.1×10^6	3.1×10^5	1×10^{-4}	no improvement
Class 2	**4d**			$C_{10}H_{21}$ [d]		1	7.2×10^5	2.4×10^5	1×10^{-3}	no improvement
symmetrically substituted PPVs	**4e**			C_8H_{17} [e]		1	5.5×10^5	1.3×10^5	9×10^{-4}	no improvement
with branched alkyl chains	**4f**	CH_3	$C_{10}H_{21}$ [d]	$C_{10}H_{21}$ [d]	0.5	0.5	7.0×10^5	2.1×10^5	1×10^{-3}	no improvement
	4g	CH_3	C_5H_{11} [f]	$C_{10}H_{21}$ [d]	0.06	0.94	6.8×10^5	2.2×10^5	1×10^{-3}	no improvement
	4h	CH_3	C_5H_{11} [f]	$C_{10}H_{21}$ [d]	0.08	0.92	7.3×10^5	2.2×10^5	1×10^{-3}	no improvement
	4i	CH_3	C_8H_{17} [e]	C_8H_{17} [e]	0.5	0.5	1.3×10^5	4.2×10^4	7×10^{-4}	no improvement
Class 3	**4j**	*n*-C_8H_{17}	*n*-C_8H_{17}	*n*-$C_{14}H_{29}$	0.5	0.5	3.8×10^5	1.3×10^5	3×10^{-3}	6×10^{-3}
symmetrically substituted PPVs	**4k**	*n*-$C_{11}H_{23}$	*n*-$C_{11}H_{23}$	*n*-$C_{15}H_{31}$	0.5	0.5	6.6×10^5	2.0×10^5	3×10^{-3}	6×10^{-3}
with linear alkyl chains	**4l**	*n*-C_8H_{17}	*n*-C_8H_{17}	*n*-$C_{18}H_{37}$	0.5	0.5	5.1×10^5	1.3×10^5	6×10^{-3}	no improvement
	4m	*n*-$C_{10}H_{21}$	*n*-$C_{10}H_{21}$	*n*-$C_{18}H_{37}$	0.5	0.5	8.9×10^5	2.7×10^5	2×10^{-3}	6×10^{-3}
	4n	*n*-$C_{11}H_{23}$	*n*-$C_{11}H_{23}$	*n*-$C_{18}H_{37}$	0.5	0.5	1.4×10^6	7.4×10^5	2×10^{-3}	1×10^{-2}
	4o	*n*-$C_{12}H_{25}$	*n*-$C_{12}H_{25}$	*n*-$C_{18}H_{37}$	0.5	0.5	1.0×10^6	3.0×10^5	2×10^{-3}	7×10^{-3}
	4p	*n*-$C_{14}H_{29}$	*n*-$C_{14}H_{29}$	*n*-$C_{18}H_{37}$	0.5	0.5	9.5×10^5	3.2×10^5	2×10^{-3}	7×10^{-3}

[a] Calculated from gel-permeation chromatography (GPC) measurements carried out by high-temperature GPC at 140 °C, using 1,2,4-trichlorobenzene as the solvent and narrow-molecular-weight-distribution polystyrene standard samples as reference. [b] Mobility values were determined in the linear operating regime ($V_g = -19$ V, $V_{sd} = -2$ V) [c] Annealing was performed under vacuum (10^{-4} mbar) at 110 °C for 5 min. [d] $C_{10}H_{21}$: 3,7-dimethyloctyl. [e] C_8H_{17}: 2-ethylhexyl. [f] C_5H_{11}: 3,3-dimethylpropyl.

zene onto OFET test substrates with a bottom-contact configuration. Heavily doped silicon was used as the gate electrode, with a hexamethyldisilazane (HMDS)-treated 200 nm-thick layer of thermally oxidized SiO_2 as the gate-insulating layer. Gold was thermally evaporated and patterned to form interdigitated source and drain contacts. All but the stability measurements were performed at 40 °C in air/light using devices with a channel length, L, of 10 μm and a channel width, W, of 20 mm. Stability measurements were measured at 22 °C in air/dark using the same device geometry.

Field-effect mobilities (Table 1) were determined in the linear regime of operation (gate voltage, V_g, of –19 V, and source–drain voltage, V_{sd}, of –2 V). When $V_g \gg V_{sd}$ the source–drain current varies linearly with V_g and the field-effect mobility can then be calculated from the transconductance:[16]

$$\mu = \frac{\partial I_{sd}}{\partial V_g} \frac{L}{WC_i V_{sd}} \quad (1)$$

where L is the channel length, W is the channel width, and C_i is the capacitance of the insulator per unit area.

The PPVs synthesized in this work can be classified into three groups, based on the substitution pattern of the phenyl ring and the nature of the side chains (Table 1). The first class comprises unsymetrically substituted PPVs, in which R^1 and R^2 are different linear or branched alkyl chains. Examples are the widely studied OC_1C_{10}–PPV **4a**, and MEH-PPV **4b**. The second class includes symmetrically substituted PPVs with branched alkyl chains or copolymers thereof. The third class is made up of symmetrical substituted PPVs with linear alkyl chains.

First we compared the electrical performance of unsymmetrically substituted PPVs of class 1 with the symmetrically substituted PPVs of class 2. Values of about 10^{-3} $cm^2 V^{-1} s^{-1}$ for the charge-carrier mobility were found for the symmetrically substituted PPVs, which is about a factor three higher than for the unsymetrically substituted PPVs of class 1. This can be explained by a higher degree of regularity of the former and likely a better ordering in the solid state, resulting in a higher mobility. Phase-imaging scanning force microscopy of these polymers has shown that the molecular structure of unsymmetrical **4a** is dominated by spiraling chains and a low degree of aggregation. In contrast, for symmetrically substituted **4d**, aligned individual chains and strong aggregation was observed.[17] The difference in charge-carrier mobilities between **4a** and **4d** was also reported by Blom and co-workers.[18] They also found a higher zero-field mobility in hole-only diodes for the symmetrically substituted PPV **4d**. Furthermore they observed that the energetic disorder σ in the symmetrical **4d** is significantly less and the localization length larger than in unsymmetrical **4a**.

In copolymers **4f–i** of class 2, a certain amount of unsymmetrical monomer was incorporated. Even for **4f** and **4i**, in which 50 % of the symmetrical monomer was replaced by the unsymmetrical monomer, the mobility is not significantly affected.

It has been shown that both optimization of processing (e.g., annealing of the semiconductor[19,20]), and optimization of the transistor configuration[21] (e.g., surface alignment layers,[22] choice of the gate insulator[23]) can further improve the performance of OFETs. Thermal annealing of semiconductors like OC_1C_{10}–PPV **4a** and MEH-PPV **4b** at temperatures beyond the glass-transition temperature (T_g) results in significant changes in the photoluminescence (PL) spectra.[19] The observed red-shift was related to emissions from interchain species, such as aggregates or excimers.[24] Attempts to improve the electrical performance of PPVs from class 1 and 2 in devices by annealing in vacuum over a temperature range of 80–200 °C failed in our case. No significant improvement of the mobility upon annealing was observed.

The third class of alkoxy-PPVs (**4j–p**) studied here are random copolymers consisting of two symmetrically substituted monomers in a 1:1 ratio. In this case, linear alkyl chains instead of the branched alkyl chains in class 2 were used. These materials can be still processed from (e.g., chlorobenzene) solution into homogeneous thin films by means of spin-coating or knife-casting. They do, however, show a much stronger tendency to form gels or aggregates upon standing at room temperature than materials from class 1 and 2 under identical conditions, indicating strong interchain interactions. All these copolymers exhibit mobilities in the range of $2–3 \times 10^{-3}$ $cm^2 V^{-1} s^{-1}$ after spin-coating. These values for the charge-carrier mobility exceed those obtained for other PPVs reported so far. Devices based on these copolymers were also subjected to a thermal treatment. For this purpose, pristine samples were heated for 5 min at a given temperature, cooled down to 40 °C and measured at this temperature. A typical example of such an annealing experiment for bis-OC_{12}–bisOC_{18}–PPV (**4o**) is depicted in Figure 1.

As can be seen the mobility after spin-coating exhibits a value of 2×10^{-3} $cm^2 V^{-1} s^{-1}$ at 40 °C. Annealing of the device at a temperature of 80 °C results in a two-fold increase to

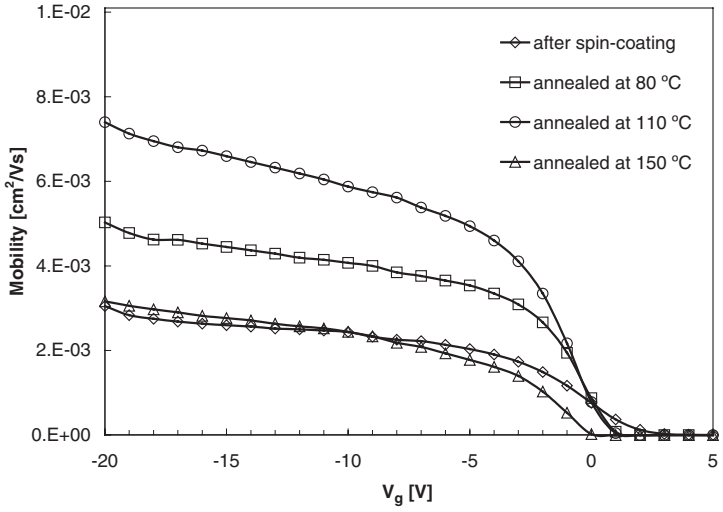

Figure 1. Mobility curves of **4o** before and after annealing (measured in air/light at 40 °C).

4×10^{-3} $cm^2 V^{-1} s^{-1}$. On going to an annealing temperature of 110 °C, the mobility further increases to 7×10^{-3} $cm^2 V^{-1} s^{-1}$. Annealing temperatures above 110 °C again lower the mobility. Apparently, an annealing temperature around 110 °C is the optimum for these PPVs.[25]

Figure 2 shows the transfer characteristics of an annealed sample of bisOC$_{11}$–bisOC$_{18}$–PPV **4n**. This material has a mobility of 10^{-2} $cm^2 V^{-1} s^{-1}$ and a current modulation of more than 10^5, when measured in air and light.[26] According to the best of our knowledge, this material displays the highest mobility of a solution-processable PPV derivative in an OFET.

In order to study the ambient stability of these PPV OFETs, devices were annealed for 5 min at 110 °C under vacuum, cooled to 22 °C, and exposed to air. The relative humidity during the stability tests varied between 50–70 %. The transfer characteristics were measured at regular time intervals, using the standard device geometry ($L = 10$ μm, $W = 20$ mm) at 22 °C and a V_{sd} of –20 V. Figure 3 shows a typical example of the ambient stability of **4n** as a function of time.

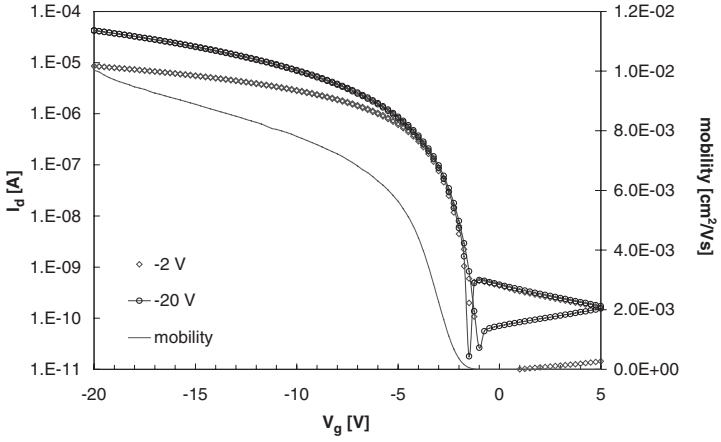

Figure 2. Current–voltage and mobility curves of **4n** after annealing at 110 °C (measured in air/light at 40 °C).

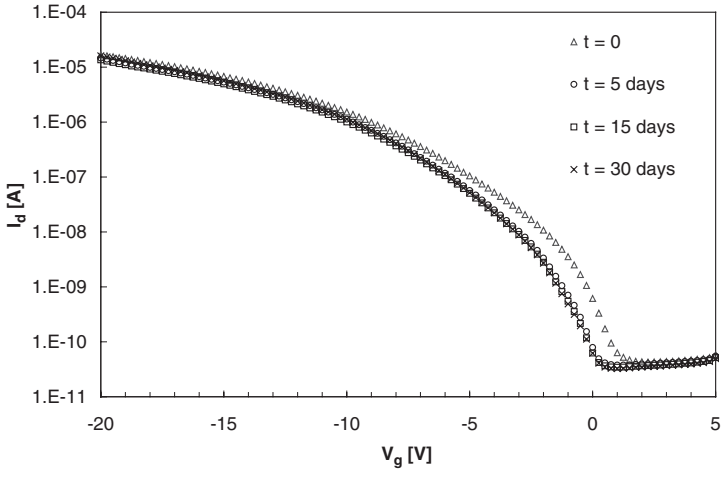

Figure 3. Transfer chracteristics of **4n** as a function of time. $V_{sd} = -20$ V, $T = 22$ °C, devices were stored in air and in the dark.

It can be seen that the initial high on/off ratio ($> 10^5$) of the OFET device remains nearly constant, even after having been stored for thirty days in humid air. These results show that PPVs like **4n** exhibit an excellent stability against p-doping by atmospheric oxygen. In addition, the device performance is not affected by humidity. The mobilities displayed by these materials are comparable with values typically obtained for regioregular head-to-tail poly(3-hexyl thiophene). However, in contrast to those made using P3HT, transistors made from PPVs do not show any significant change in the electrical performance when stored in air and under dark conditions.

3. Conclusion

In this paper we have reported on the influence of structural engineering and processing of several solution-processable PPVs on the electrical performance in FETs. Based on the substitution pattern and nature of the side chains, the respective PPVs were divided into three classes. Unsymmetrically substituted PPVs display mobilities in the region of 10^{-4} $cm^2 V^{-1} s^{-1}$. The higher degree of main-chain regularity of the symmetrically substituted PPVs of class 2 resulted in an increase of the mobility of about one order of magnitude. The combination of a high degree of main-chain regularity with non-branched side chains in class 3 finally led to mobilities of several times 10^{-3} $cm^2 V^{-1} s^{-1}$. These mobilities could be further improved up to 10^{-2} $cm^2 V^{-1} s^{-1}$ by annealing the polymers at 110 °C. In addition, these devices display an excellent stability in air and in the dark. No change in the electrical performance was observed, even after storage for thirty days in humid air. The combination of high mobility and good stability in air opens the way for a wide scope of applications in plastic electronics.

4. Experimental

General Procedure for the Synthesis of 1,4-Bis(alkoxy)benzenes ***2***: A mixture of hydroquinone (18.71 g, 0.17 mol) and powdered KOH (28.1 g, 0.425 mol) in dimethyl sulfoxide (DMSO) (400 mL) was degassed and stirred under nitrogen for 1 h. Subsequently, bromoundecane (100 g, 0.43 mol) was added and stirred for 3 h under nitrogen. The mixture was poured into ice–water and the white precipitate obtained was filtered off, washed with water and ethanol, dried, and subsequently recrystallized in ethanol. 61.9 g (87 %) of **2** was obtained as white crystals. ^{1}H NMR ($CDCl_3$): δ 0.88 (t, 6H, CH_3, J = 6.3 Hz), 1.2–1.35 (m, 28H, $-CH_2-$), 1.42 (m, 4H, $OCH_2CH_2CH_2$), 1.75 (q, 4H, OCH_2CH_2), 3.89 (t, 4H, OCH_2, J = 6.6 Hz), 6.82 (s, 4H, ar H).

General Procedure for the Synthesis of 1,4-Bis(alkoxy)-2,5-bis(chloromethyl)benzenes ***3***: A 31.40 g (75 mmol) sample of diundecyloxybenzene and 6.22 g (207 mmol) of paraformaldehyde were placed in a 500 mL three-necked flask fitted with a magnetic stirrer, reflux condenser, thermometer, and dropping funnel. Under nitrogen, 35 mL dioxane and 36 mL (429 mmol) of 37 % HCl were added. A 72 mL (765 mmol) aliquot of acetic anhydride was then added dropwise at such a rate that the internal temperature did not exceed 70 °C. The mixture was stirred

for 18 h at 70–75 °C. It was then cooled to room temperature while stirring; a light-colored solid crystallized. The reaction mixture was mixed with 70 mL of saturated sodium acetate solution, and 50 mL of 25 % NaOH was then added dropwise at such a rate that the internal temperature did not exceed 50 °C. The mixture was then cooled with an ice bath while stirring rapidly. The off-white solid was filtered off and washed with 200 mL of H_2O. The solid was dissolved in chloroform (35 mL) and treated with 3×300 mL of H_2O; the pH was 5. The organic phase was dried over $MgSO_4$ and filtered. The filtrate was evaporated and crystallized once from ethyl acetate (EtOAc) and once from toluene to give the title compound as white crystals (29.4 g, 76 %). ^{1}H NMR ($CDCl_3$): δ 0.88 (t, 6H, CH_3, J = 6.4 Hz), 1.2–1.4 (m, 28H, $-CH_2-$), 1.47 (m, 4H, $OCH_2CH_2CH_2$), 1.79 (q, 4H, OCH_2CH_2), 3.98 (t, 4H, OCH_2, J = 6.6Hz), 4.63 (s, 4H, CH_2Cl), 6.91 (s, 2H, ar H).

General Procedure for Polymerization: A 500 mL three-necked flask fitted with a reflux condenser and dropping funnel was charged with 0.83 g 2,5-bis(chloromethyl)-1,4-bis(undecyloxy)benzene (1.60 mmol), 1.14 g 2,5-bis(chloromethyl)-1,4-bis(octadecyloxy)benzene (1.60 mmol) and dry 1,4-dioxane (250 mL), and the solution was degassed by passing nitrogen through it for about 15 min. The solution was heated to 98 °C with an oil bath. A 0.90 g (8 mmol, 2.5 equiv.) sample of potassium *tert*-butoxide, dissolved in 10 mL of 1,4-dioxane, was added dropwise to the reaction solution from the dropping funnel over a period of 2 min. During this addition, the reaction mixture changed color from colorless, via greenish, to yellow–orange, and the viscosity increased significantly. After the addition was complete, the mixture was stirred further for about 5 min at 98 °C; 0.90 g of potassium *tert*-butoxide (8 mmol, 2.5 equiv.) in 10 mL of dry 1,4-dioxane was then added over a period of 1 min, and stirring was continued for 2 h at 96–98 °C. Upon cooling the solution to 50 °C, the solution turned dark red and the polymer started to precipitate. The reaction mixture was finally mixed with 1.5 mL (1.5 equiv., based on the base) of acetic acid and stirred further for 20 min. For the workup, the reaction solution was slowly poured into 500 mL of intensively stirred water. The resulting mixture was stirred further for 10 min, and the precipitated polymer was filtered off. This was washed with 100 mL of methanol and dried under reduced pressure at room temperature. The crude polymer was purified by dissolving it in 150 mL of chlorobenzene (85 °C oil bath) and precipitating the polymer by the dropwise addition in 1000 mL of methanol. After washing with 200 mL of methanol, it was dried at room temperature under reduced pressure. This procedure was repeated once more using 150 mL hot chlorobenzene/850 mL of methanol. This procedure was repeated once more using 150 mL of chlorobenzene/850 mL of acetone. A 1.21 g (70 %) sample of poly[(2,5-bisundecyloxy-*p*-phenylenevinylene)-*co*-(2,5-bisoctadecyloxy-*p*-phenylenevinylene)] was obtained as a dark-red solid. ^{1}H NMR ($C_2D_2Cl_4$, 373 K): δ 0.92–0.98 (br t, 12H, CH_3), 1.25–1.55 (br m, 84H, $-CH_2-$), 1.55–1.7 (br m, 8H, $OCH_2CH_2CH_2$), 1.85–2.05 (br m, 8H, OCH_2CH_2), 3.6–4.4 (br m, 8H, OCH_2), 6.5–8.0 (br m, 4H, ar H). $M_w = 1\,445\,000$ g mol^{-1}, number-average molecular weight, $M_n = 744\,350$ g mol^{-1}.

Processing and Electrical Characterization: Characterization was performed under ambient conditions. Films were prepared by spin-coating a 0.3 wt.-% solution of PPV in chlorobenzene at a speed of 2000 rpm (revolutions per minute) for 30 s. Transistor measurements were performed at 40 °C in air/light using a HP4156B semiconductor parameter analyzer.

Received: September 23, 2004
Final version: November 4, 2004

[1] G. H. Gelinck, T. C. T. Geuns, D. M. de Leeuw, *Appl. Phys. Lett.* **2000**, *77*, 1487.
[2] H. E. A. Huitema, G. H. Gelinck, J. B. P. H. van der Putten, K. E. Kuijk, C. M. Hart, E. Cantatore, P. T. Herwig, A. J. J. M. van Breemen, D. M. de Leeuw, *Nature* **2001**, *414*, 599.
[3] C. J. Brabec, V. Dyakonov, J. Parisi, N. S. Sariciftci, in *Organic Photovoltaic Concepts and Realization*, Vol. 60, Springer, London **2003**.
[4] A. Assadi, C. Svensson, M. Willander, O. Inganäs, *Appl. Phys. Lett.* **1988**, *53*, 195.
[5] Z. Bao, A. Dodabalapur, A. J. Lovinger, *Appl. Phys. Lett.* **1996**, *69*, 4108.
[6] H. Sirringhaus, N. Tessler, R. H. Friend, *Science* **1998**, *280*, 1741.
[7] E. J. Meijer, C. Detcheverry, P. J. Beasjou, E. van Veenendaal, D. M. de Leeuw, T. M. Klapwijk, *J. Appl. Phys.* **2003**, *93*, 4831.
[8] B. Ong, Y. Wu, L. Jiang, P. Liu, K. Murti, *Synth. Met.* **2004**, *142*, 49.
[9] B. Ong, Y. Wu, P. Liu, S. Gardner, *J. Am. Chem. Soc.* **2004**, *126*, 3378.
[10] The authors state that humidity has an effect on device performance; stability measurements were therefore performed in dry air.
[11] www.research.philips.com/InformationCenter/Global/FPressRelease.asp? 1ArticleId=2701&1NodeId=929
[12] C. Tanase, E. J. Meijer, P. W. M. Blom, D. M. de Leeuw, *Phys. Rev. Lett.* **2003**, *91*, 216 601-1.
[13] H. G. Gilch, *J. Polym. Sci., Part A: Polym. Chem.* **1966**, *4*, 1337.
[14] H. Spreitzer, W. Kreuder, H. Becker, H. Schoo, R. Demandt, *PCT Patent Application WO 9 827 136*, **1996**.
[15] H. Becker, H. Spreitzer, K. Ibrom, W. Kreuder, *Macromolecules* **1999**, *32*, 4925.
[16] A. R. Brown, C. P. Jarrett, D. M. de Leeuw, M. Matters, *Synth. Met.* **1997**, *88*, 37.
[17] M. Kemerink, J. K. J. van Duren, P. Jonkheijm, W. F. Pasveer, R. A. J. Janssen, H. W. M. Salemnink, J. H. Wolter, *Nano Lett.* **2003**, *3*, 1191.
[18] H. C. F. Martens, P. W. M. Blom, H. F. M. Schoo, *Phys. Rev. B* **2000**, *61*, 7489.
[19] J. Liu, T. F. Guo, Y. Yang, *J. Appl. Phys.* **2002**, *91*, 1595.
[20] J. M. Warman, G. H. Gelinck, M. P. de Haas, *J. Phys.: Condens. Matter* **2002**, *14*, 9935.
[21] The improvement of the transistor configuration has not been done yet. This will be subject of future investigations.
[22] H. Sirringhaus, R. J. Wilson, R. H. Friend, M. Inbasekaran, W. Wu, E. P. Woo, M. Grell, D. D. C. Bradley, *Appl. Phys. Lett.* **2000**, *77*, 406.
[23] J. Veres, S. D. Ogier, S. W. Leeming, D. C. Cupertino, S. M. Khaffaf, *Adv. Funct. Mater.* **2003**, *13*, 199.
[24] T.-Q. Nguyen, I. B. Martini, J. Liu, B. J. Schwartz, *J. Phys. Chem.* **2000**, *104*, 237.
[25] It should be noted that annealing has no influence on the off-current.
[26] The current at positive gate bias is dominated by parasitic currents due to the unpatterned semiconductor and interdigitated electrodes.

